ROYAL SOCIETY OF CHEMISTRY

PAPER

Check for updates

Fabrication and evaluation of melamine-formaldehyde resin crosslinked PVA composite coating membranes with enhanced oxygen barrier properties for food packaging

Qingmei Zhu,[abc] Xianghui Wang,[bc] Xiuqiong Chen,[abc] Changjiang Yu,[abc] Qi Yin,[bc] Huiqiong Yan *[abc] and Qiang Lin (ID) *[abc]

Since PVA membrane is of limited use for food packaging applications in moist conditions, polyvinyl alcohol/melamine-formaldehyde resin (PVA/MF) composite coating membranes with various contents of MF were fabricated by a chemical crosslinking method to reduce the sensitivity of PVA to moisture. The morphology, chemical structure, thermal and mechanical properties of the resultant PVA/MF composite coating membranes were characterized by scanning electron microscopy (SEM), FT-IR spectrometer, X-ray diffraction (XRD), thermal gravimetric analysis (TGA), differential scanning calorimeter (DSC) and universal testing machine. In addition, their hazes and OTRs were also measured as a function of MF content. Experimental results showed that −OH in the molecular chain of MF and PVA could be crosslinked at room temperature to form a dense polymeric structure, resulting in the increase in viscosity and the decline in water absorption. The incorporation of MF into PVA gave rise to the enhancement of crosslinking through the C−O−C bonding and strong interface interaction between MF and PVA that was beneficial to improving its thermal stability, mechanical properties and barrier properties. Furthermore, the PVA/MF composite coating membranes exhibited superior transparency due to their good leveling and wettability on both BOPET and PLA substrates. The moisture resistance and barrier properties of the MF/PVA composite coated BOPET and PLA membranes under high humidity conditions have been greatly improved, and the oxygen transmission rates (OTRs) under 75% RH could still remain at about 1.0 cm^3 per m^2 per day. These characteristics of the PVA/MF composite coating membranes have made them exhibit widespread application prospects for coating membranes in the food packaging field.

1 Introduction

The oxygen present in food packaging can cause rapid food deterioration due to the fast oxidation of fats or vitamins existing in the food (*i.e.* oxidative rancidity) or the promotion of the growth of aerobic bacteria, yeasts and molds.[1] Therefore, oxygen barrier properties are important for food packaging materials, especially for foods with high sugar and high fat.[2] With the rising awareness of traditional high-barrier materials, such as polyvinyl dichloride (PVDC) and aluminum foil

materials that are not environmentally friendly, the demand for environmentally friendly, transparent, and high-barrier flexible packaging materials is increasing. In commercial practice, other than EVOH multi-layer co-extrusion film,[3,4] SiOx/AlOx coating,[5–7] poly(vinyl alcohol) (PVA)[8–11] with good transparency, excellent oxygen barrier properties and desirable film-forming has become an ideal candidate for flexible packaging applications.

PVA, as a water-soluble polymer, has low oxygen permeability due to its semi-crystalline structure and strong intermolecular interaction, but when the relative humidity (RH) exceeds 75%, the oxygen permeability of PVA increases exponentially.[12,13] In this case, PVA coatings are often coated onto polyolefin membranes such as biaxially oriented polyethylene tere-phthalate (BOBOPET), biaxially oriented polypropylene (BOPP) and biaxially oriented nylon (BONylon) through the waterborne coating process (the thickness of the PVA coating is about 1 μm) in the field of industrial flexible packaging. Then these PVA coatings are printed and further laminated with sealant film

[a]Key Laboratory of Tropical Medicinal Resource Chemistry of Ministry of Education, College of Chemistry and Chemical Engineering, Hainan Normal University, Haikou 571158, Hainan, P. R. China. E-mail: yanhqedu@163.com; Tel: +86 0898 65884995

[b]Key Laboratory of Natural Polymer Functional Material of Haikou City, College of Chemistry and Chemical Engineering, Hainan Normal University, Haikou 571158, Hainan, P. R. China. E-mail: linqianggroup@163.com; Tel: +86 0898 65889422

[c]Key Laboratory of Water Pollution Treatment & Resource Reuse of Hainan Province, College of Chemistry and Chemical Engineering, Hainan Normal University, Haikou 571158, Hainan, P. R. China

such as linear low-density polyethylene (LLDPE) film or casted polypropylene (CPP) film, which aims to sandwich the PVA coating between two films with good water vapor barrier properties to maintain low oxygen transmission rate (OTR) under high humidity. In general, foods such as biscuits and bread require an OTR of less than 10 cm^3 per m^2 per day at 75% RH or higher humidity, while coffee and high-sugar and high-fat snack foods require an OTR of less than 1.0 cm^3 per m^2 per day at 75% RH or higher humidity.[14,15] However, the present problem is that the coated membrane may be put on hold for several months before the next printing and lamination process, and the exposed PVA coating is prone to coating anti-adhesion due to its hydrophilicity, which reduces its oxygen barrier properties.

In order to reduce the sensitivity of PVA to moisture, many attempts have been made, one of which is to construct PVA–nanocomposite materials. For example, composite materials prepared with layered materials, MMT[8,16,17] or graphene oxide[9,18,19] have excellent gas barrier properties due to the fact that nanosheets can be intercalated in the PVA coating. The tortuous path of oxygen permeation caused by the orderly arrangement of the nanosheets in the PVA–nanocomposite helps to improve the gas barrier properties of the coating materials. However, the dispersibility of nanomaterials in PVA and the complicated preparation process of nanocomposites still become an urgent problem.[10,11] Another convenient and efficient method is to chemically cross-link PVA. PVA can undergo chemical reactions similar to other secondary polyols, and esterification of PVA can be carried out with a number of compounds to improve the properties of PVA coating such as solvent resistance, mechanical properties and permeability, *etc.*[20–22] Typical crosslinkers of PVA include carboxylic acids and their analogs,[23,24] various aldehydes,[25,26] and other chemical crosslinking agents.[27] Among them, the common crosslinking agents used in food packaging materials are aldehydes, such as glutaraldehyde and glyoxal[8,9] as well as boric acid,[28] *etc.*, focusing on the effects of crosslinking on PVA membrane properties such as water absorption, barrier properties and mechanical properties. Previous studies have shown that the melamine-formaldehyde (MF) resin crosslinking agent can achieve an ether exchange reaction with the hydroxyl group on the polymer under acidic conditions. In addition, the MF itself will undergo a complex self-crosslinking reaction,[29–32] and the coatings made from the reaction of MF resins and hydroxyl polymers can improve their chemical resistance, hardness and other properties for the application in the coating industry. MF resins have also been reported as crosslinking agents for PVA, but they are mainly used in the field of electrospinning and preparation of aerogels.[33–36] However, there are few systematic reports on MF crosslinked PVA as a barrier coating in food flexible packaging.

In this study, the PVA/MF composite coating membranes with various contents of MF were fabricated by chemical crosslinking method to decrease the sensitivity of PVA to moisture. The morphology, chemical structure and properties of the resultant PVA/MF composite coating membranes after heat treatment were characterized by scanning electron

microscopy (SEM), FT-IR spectrometer, X-ray diffraction (XRD), thermal gravimetric analysis (TGA), differential scanning calorimeter (DSC) and universal testing machine. Meanwhile, their hazes and OTRs were also measured as a function of MF content. The objective of the present study was to explore the application of improving the humidity sensitivity of PVA coatings as high barrier coatings on BOPET and PLA substrates in the field of food packaging.

2 Experimental procedure

2.1 Materials

Polyvinyl alcohol with number-average degree of polymerization of 1700 (PVA, degree of hydrolysis = 98.9–99%) was purchased from Changchun Chemical Co., Ltd. (Changchun, China). Melamine-formaldehyde resin (MF, CYMEL 385, a partially methylated melamine formaldehyde resin with alkoxy, methylal, and amino reactive groups, whose monomer molecular structural formula is presented in Fig. 1, at a concentration of 79% in water) was provided by ALLNEX.[37] BOPET film (a thickness of 12 μm) with the oxygen transmission rate (OTR) of 132.55 cm^3 per m^2 per day was obtained from Guangdong Weifu Packaging Material Co., Ltd. (Guangzhou, China). PLA film (a thickness of 20 μm) with the OTR of 980.60 cm^3 per m^2 per day was bought from Shandong Shenghe Plastic Development Co., Ltd. (Heze, China). Other reagents were purchased from Aladdin Chemical Reagent Co., Ltd. (Shanghai, China), and they were of analytical grade without further purification.

2.2 Methods

2.2.1 Fabrication of PVA/MF composite coating membranes. A certain amount of PVA was dissolved in deionized water by stirring at 95–98 °C to form a 6 wt% PVA solution, and then the solution was cooled to 25 °C. MF in various amounts of 0–10 wt% based on PVA weight was added to the PVA solution under stirring. Afterwards, the pH of the resultant solution was adjusted to 3.0 by the addition of 0.5 mol L^{-1} hydrochloric acid, and then it was stirred at 25 °C for 24 h to obtain the MF crosslinked PVA blend solutions. Finally, each blend solution was cast onto a glass plate using a casting knife with a gap of 300 μm, and the glass plate was dried in a vacuum oven at 70 °C for 12 h. The membranes thickness was maintained at about 20 ± 2 μm for the further characterization.

2.2.2 Preparation of PVA/MF composite coated BOPEF and PLA membranes. The surfaces of the PLA and the BOPET films
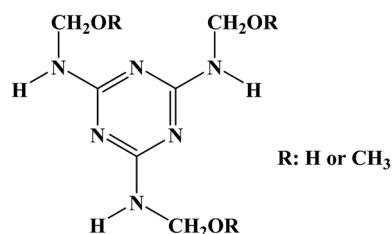

Fig. 1 Monomer molecular structural formula of melamine-formaldehyde resin.

Paper

RSC Advances

were corona treated using the laboratory corona processor (BD-20AC Laboratory Corona Treater), making the surface tensions of the two substrates were greater than 38 dyn cm^{-1}. The above MF crosslinked PVA blend solutions were respectively coated onto BOPEF and PLA films to form the PVA/MF composite coated BOPEF membranes and PLA membranes by the use of No. 7 RDS Mayer coating bar (Germany) after the corona discharge treatment. The coating process was repeated several times to obtain sufficiently thick coatings for the evaluation of their OTRs and hazes. After being completely dried, the coating thickness of PVA/MF composite was about 1 μm.

2.2.3 Characterization of PVA/MF composite coating membranes. The viscosity of PVA/MF composite coating membranes was measured using a Brookfield DV-II+Pro Rotational Viscometer. The test temperature was fixed at 25 °C and the rotation speed was 60 rpm. The swelling behavior of the PVA/MF composite coating membranes (50 mm × 50 mm) was examined by immersing dry PVA/MF composite coating membranes in deionized water for a time period of 24 h. The swollen weight of the PVA/MF composite coating membranes was recorded after removal of excessive surface water by filter paper. Three parallel experiments were carried out for every sample and the mean value was taken. The swelling ratio (SR) of the PVA/MF composite coating membranes was calculated based on the weight difference between the dry and swollen samples using the following equation.

$$SR = \frac{\text{swollen sample weight} - \text{dry sample weight}}{\text{dry sample weight}} \times 100\% \quad (1)$$

The morphology of the samples was observed by scanning electron microscope (SEM). SEM observation was executed using a Hitachi S-3000N (Japan) scanning electron microscope after fixing the samples on a brass holder and coating them with gold. The FT-IR spectroscopy of the samples were conducted using a Bruker Tensor 27 FT-IR spectrophotometer (Germany).

About 2 mg of the sample was mixed with 100 mg of KBr, dried with an infrared lamp and then compressed to semitransparent disks for spectroscopic analysis to determine the composition of samples' functional groups. The samples were scanned from 400 to 4000 cm^{-1} at a resolution of 4 cm^{-1}. XRD analyses of samples were performed on a Bruker AXS/D8 advance diffractometer (Germany) using Cu-Kα (λ = 0.154 nm), which was operated at 40 kV and 100 mA in step scan mode at a scanning speed of 0.02° s^{-1}. X-ray diffraction measurements were performed over a 2θ range of 5°–60°. TGA of samples were carried out on a TA Q600 Thermal Analyzer in air at a heating rate of 10 °C min^{-1} from 30 °C to 700 °C. DSC of samples were conducted with a NETZSCH 214 polyma differential scanning calorimeter (Germany) in the temperature range of 30–250 °C at a heating rate of 20 °C min^{-1} under nitrogen atmosphere. The mechanical property of the samples was determined using a ZwickRoell universal testing machine (Germany) with the applied standard of ISO 527-1:2012. The samples were cut into rectangular strips of 15 mm × 200 mm for mechanical testing. The tensile tests were conducted in the controlled strain rate mode with a preload of 1 N and a strain ramp rate of 10.0% per min. A total of five replicates were averaged for each sample.

2.2.4 Hazes and OTRs measurement of PVA/MF composite coated BOPEF and PLA membranes. Hazes of the PVA/MF composite coated BOPEF membranes and PLA membranes were evaluated using a BYK-Gardner haze-Gard plus instrument (Columbia, MD). The haze measurement provides the amount of wide-angle scattering, which is the percentage of light that deviates from the incident beam by more than 2.5° as specified by ASTM D1003, membranes that have a large haze value (10%) tend to have a milky appearance. The OTRs of the PVA/MF composite coated BOPEF membranes and PLA membranes were measured using a MOCON Oxtran-2/22 instrument (Modern Controls, Minneapolis, USA), following the ASTM Standard Method D 3985 at 25 °C and four levels of relative humidity (RH) ranging from 0 to 90%.[38]
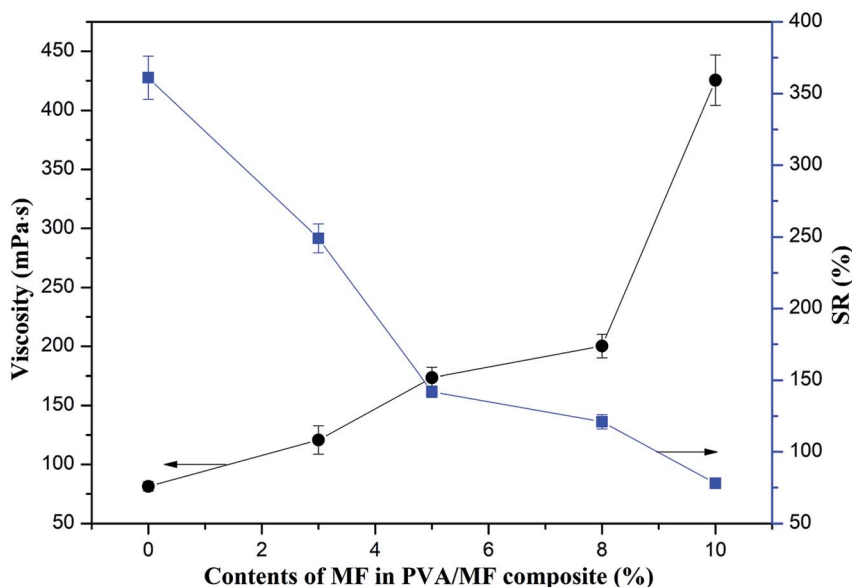

Fig. 2 Viscosity and SR of PVA/MF composite coating membranes.

3 Results and discussion

3.1 Chemical crosslinking and morphology of the PVA/MF composite coating membranes

In this work, a water-soluble and partially methylated MF was selected as the crosslinking agent, which had good compatibility with PVA. The hydroxymethyl and methoxy groups in MF would crosslink with the hydroxyl groups on PVA under acidic conditions, and the complex self-crosslinking reactions would also occur to achieve the chemical crosslinking between MF and PVA.[29,30,36]

The viscosity of PVA/MF blend solutions after chemical crosslinking at room temperature for 12 h is shown in Fig. 2. Compared with the viscosity of pure PVA solution, with the increase of MF addition, the viscosity of PVA/MF blend solutions gradually rose from 81.4 mPa s to 425.6 mPa s. In addition, the composite coating membranes formed by casting the PVA/MF blend solutions onto a glass plate showed good transparency after being dried at 70 °C for 12 h. It can be observed from Fig. 2 that the swelling rate (SR) of the pure PVA membrane was 361%, but the SR of the composite coating membranes crosslinked by MF was significantly reduced. PVA was a hydrophilic polymer with the presence of numerous pores in its dry membrane, which was prone to absorbing water molecules to swell, whereas the reduced SR of the crosslinked PVA/MF composite coating membranes was related to the crosslink density of the polymer network structure.[24,28] These results suggested that the –OH in the molecular chain of MF and PVA could be crosslinked at room temperature to form a dense polymeric structure, resulting in the increase in viscosity and the decline in water absorption, as well as the greater the amount of MF addition, the greater the crosslinking density.
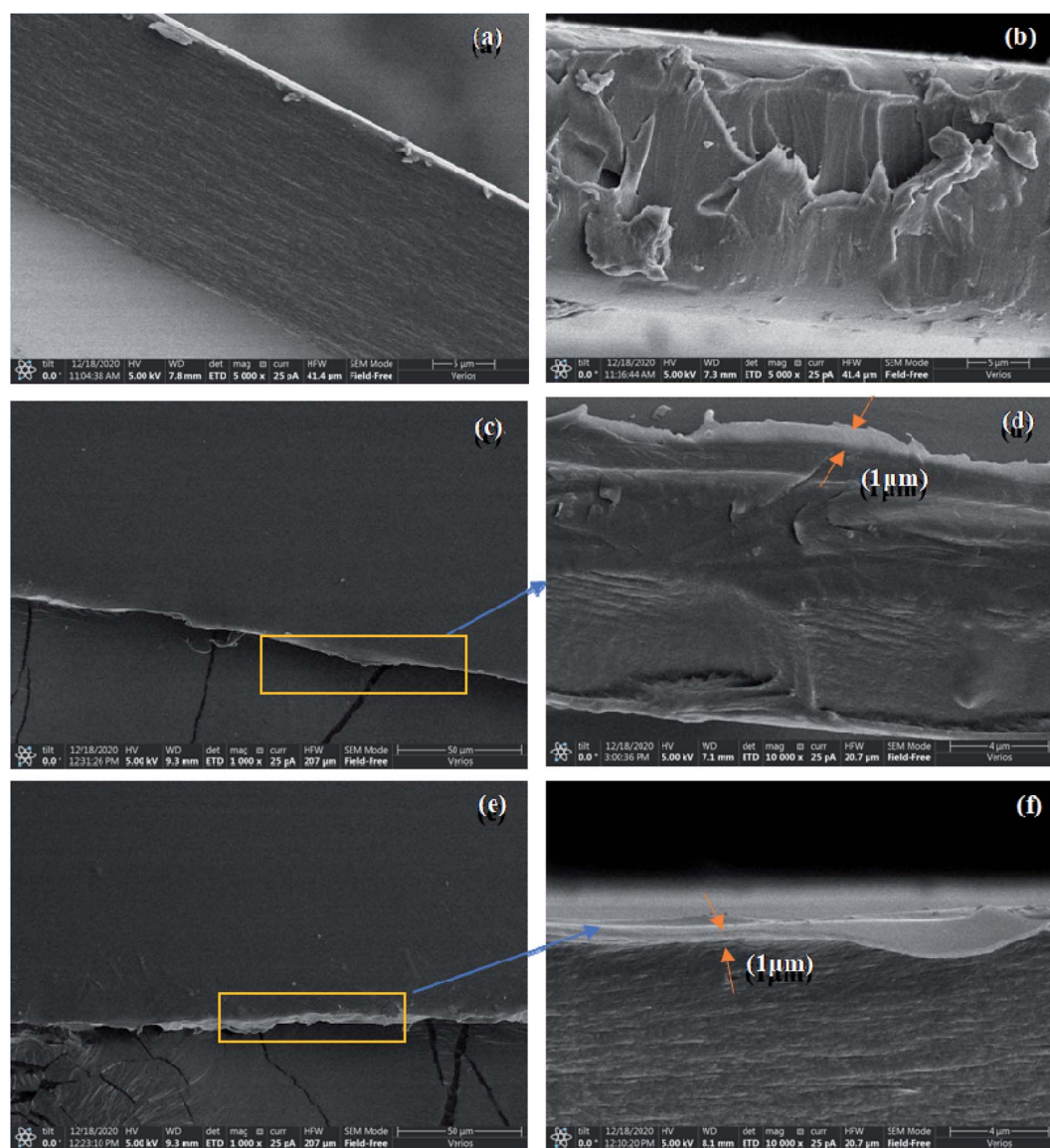

Fig. 3 SEM images of (a) fractured surface of PVA membrane, (b) fractured surface of PVA/8% MF composite coating membrane, (c) flat surface of BOPET–PVA/8% MF composite membrane, (d) fractured surface of BOPET–PVA/8% MF composite membrane, (e) flat surface of PLA–PVA/8% MF composite membrane, (f) fractured surface of PLA–PVA/8% MF composite membrane.

Paper

RSC Advances

To further observe the microscopic morphology of the PVA/MF composites and its coated membranes, SEM observation was performed on the plane and section of the resultant membranes. Fig. 3a and b display the fractured surfaces of PVA membrane and PVA/8% MF composite coating membrane. It was observed that the fractured surface of PVA was smooth and flat, while the fractured surface of PVA/8% MF composite coating membrane was rough, which was direct evidence of the chemical crosslinking between PVA and MF, and the presence of their interface interactions. It is common knowledge that the water-based coatings are required to have good wetting and leveling on the substrate in order to obtain a good coating appearance and performance. Furthermore, it can be observed from Fig. 3c and d that the flat surface of BOPET–PVA/8% MF composite membrane was very smooth because of the good film-forming properties of PVA/MF composite coating on BOPET substrate, and the coating thickness was about 1 μm. From Fig. 3e and f, the PLA–PVA/8%MF composite membrane exhibited the similar film-forming properties to the BOPET–PVA/8%MF composite membrane. This result indicated that the PVA/MF composite coating had very good leveling and wettability on both BOPET and PLA substrates by roller coating, which provided a very effective way for its packaging application.

3.2 Chemical structure of PVA/MF composite coating membranes

The chemical structure and crystal structure of PVA/MF composite coating membranes were confirmed by FT-IR spectroscopy and X-ray diffraction. As shown in Fig. 4, the broad and strong peaks appearing between 3000 and 4000 cm^{-1} were assigned to the –OH stretching vibrations of PVA, MF, PVA/5%

MF composite coating membrane and PVA/10% MF composite coating membrane. The PVA showed characteristic peaks at 2939.30, 1091.63 and 850.55 cm^{-1} which were respectively attributed to the –CH$_2$– stretching vibration and C=O stretching vibration.[9,28,33] Due to the crosslinking reaction between MF and PVA and the coating effects of PVA, the PVA/MF composite coating membranes exhibited the spectra similar to those of pure PVA without the obvious peaks of MF.[34,35] Moreover, the PVA/MF composite coating membranes displayed slight indications at 813.90 cm^{-1} which was the characteristic of triazinyl ring of melamine moiety with the increase of MF content. Meanwhile, –OH stretching vibration peak at 3330.82 cm^{-1}, C–H bending vibration peak at 653.82 cm^{-1}, and C–O–C stretching vibration peak at 1078.13 cm^{-1} became weaker and wider, which indicated the chemical reaction between MF and PVA, forming C–O–C bridges between PVA polymer chains.[28] In addition, the crosslinking reaction between MF and PVA resulted in the significant reduction of their –CH$_2$– stretching vibration peaks at 2939.30 cm^{-1} and the enhancement of their C–O–C stretching vibration peaks at 1078.13 cm^{-1}, which may be ascribed to the self-condensation between the molecules of MF to form methylene bridges and methylene ether bridges.[31] The incorporation of MF into PVA gave rise to the changes of chemical structure of PVA, such as its enhanced crosslinking and decreased hydrophilicity, and the physical properties of the PVA/MF composite coating membrane, such as thermal stability, mechanical properties and barrier properties.

The XRD patterns of PVA/MF composite coating membranes with various MF contents are shown in Fig. 5. The PVA exhibited three characteristic diffraction peaks at 11.54° (low intensity), 19.79° (high intensity) and 40.60° (very low intensity) which were respectively corresponding to the (100), (110), and (220)
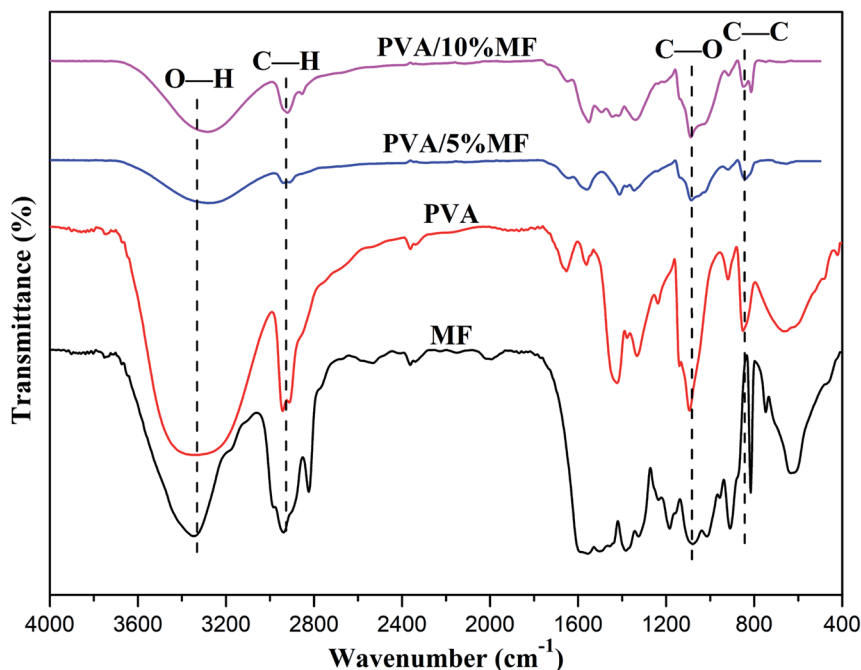

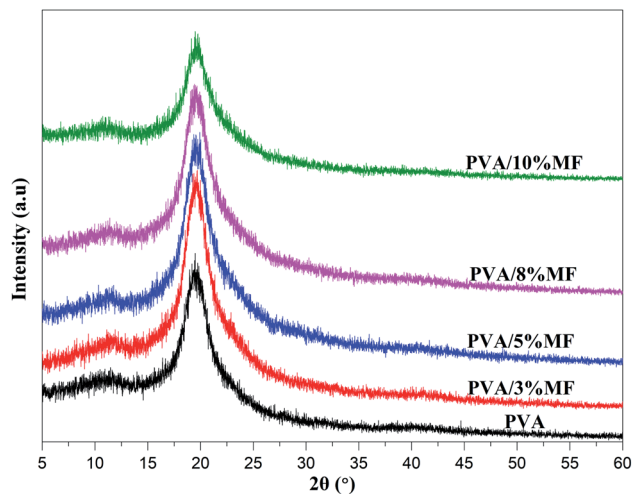Fig. 4 FT-IR spectra of PVA, MF, PVA/5% MF composite coating membrane and PVA/10% MF composite coating membrane.

**Fig. 5** XRD patterns of PVA membrane and PVA/MF composite coating membranes.

reflections.[28,34,39] Obviously, PVA/MF composite coating membranes displayed the XRD patterns similar to those of the pure PVA. When the MF addition amount was 3%, 5% and 8%, the peak intensity at $2\theta = 19.7°$ was slightly increased with the increase of MF contents, and when the MF addition amount was 10%, the peak intensity was significantly weakened, which was different from the result that many chemical crosslinkers hindered the crystallization behavior of PVA, thus making the peak intensity at $2\theta = 19.7°$ weaker. The possible reason was that when MF was added very little, MF existing in the amorphous region of PVA would not penetrate into the crystalline sequence chain of PVA. The crosslinking and curing process would not affect the crystallization behavior of PVA. MF reacted with PVA molecular chain in the amorphous area to make the molecular packing more dense and the amorphous area be reduced, improving the peak intensity at $2\theta = 19.7°$.[28,34] When the MF addition amount gradually increased, in addition to the chemical reaction between MF and PVA during the thermal curing process, there would be self-condensation between its own molecules to form methylene

bridges and methylene ether bridges,[31] consistent with the FT-IR analysis. The large three-dimensional network structure caused by self-condensation would destroy the PVA molecular packing density to enlarge the amorphous region, which would affect the chemical structure and performance of PVA.

According to the above analysis, we speculated that the chemical crosslinking of MF and PVA mainly occurred in the amorphous region of PVA, so their chemical crosslinking mode could be expressed in the following schematic diagram, as shown in Scheme 1. And the reaction mechanism of the reaction between the methoxy and hydroxymethyl groups in MF with the hydroxyl groups on PVA could be illustrated in Scheme 2.
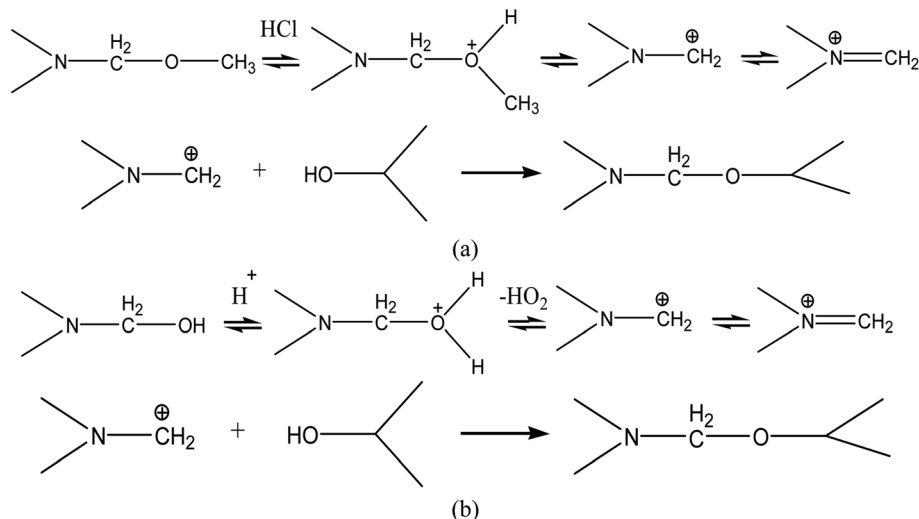
3.3 Thermal stability of PVA/MF composite coating membranes

The thermal gravity analysis (TGA) was performed to investigate the thermal stability of PVA/MF composite coating membranes. The TGA and DTG curves of PVA membrane and PVA/MF composite coating membranes are shown in Fig. 6. It can be observed that the thermal decomposition of pure PVA followed three main weight loss stages. The first stage occurred at 50–100 °C was ascribed to the removal of physically adsorbed water and bound water from the PVA.[25,40,41] The maximum rate of the second weight loss stage occurred at about 270 °C was ascribed to the dehydration, chain scission or decomposition of PVA, which was gradually thermally cracked into CO, CO_2 and H_2O, resulting in a rapid decline in their weight.[42–44] The third weight loss stage observed at around 430 °C was the decomposition of PVA by-products. Compared with PVA, PVA/MF composite coating membranes also exhibited three main weight loss stages with the different decomposition modes. The first weight loss stage observed at about 50–100 °C could be attributed to the loss of water firmly bound to the PVA structure. The broad peak at 250–500 °C was related to the ether bond formed between PVA and MF and the self-condensation of MF. Obviously, the thermal decomposition of PVA/MF composite coating membranes shifted to a high temperature range in comparison with PVA, which indicated that even a small amount of MF was very effective to improve the thermal stability of PVA. The
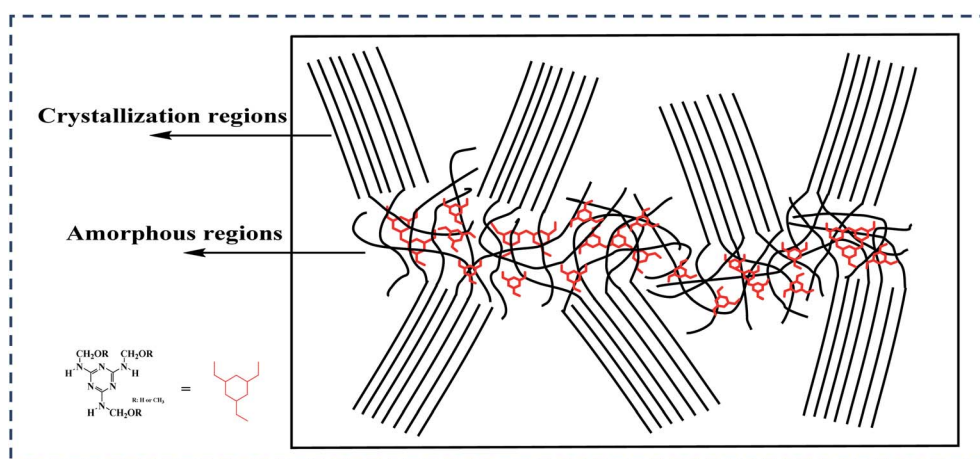
Scheme 1 Schematic representation of chemical crosslinking between PVA and FM.

Scheme 2 The reaction between (a) the methoxy groups and (b) the hydroxymethyl groups of MF with the hydroxyl groups on PVA.
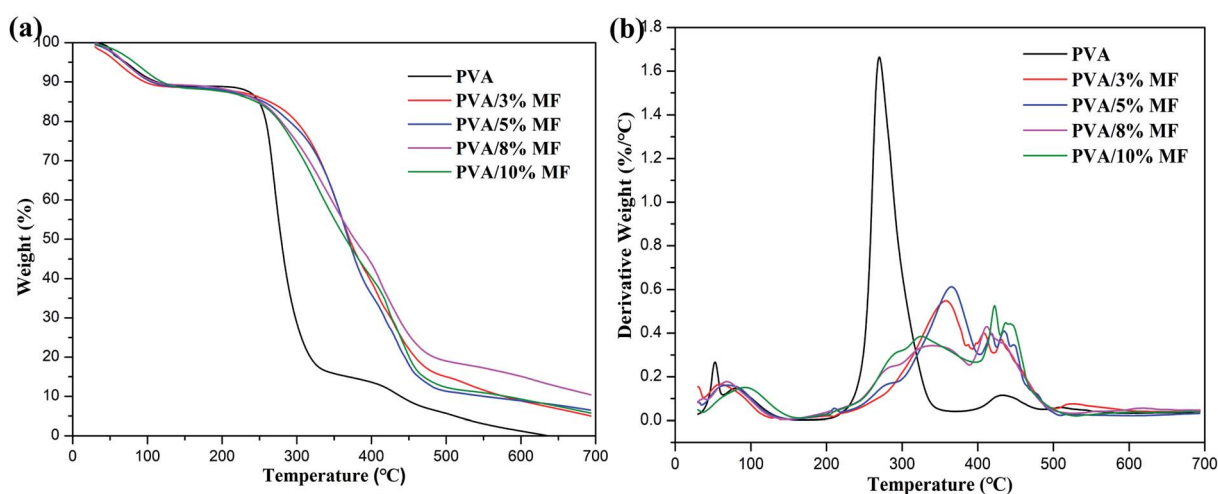

Fig. 6 (a) TGA and (b) DTG curves of PVA membrane and PVA/MF composite coating membranes.

enhancement of thermal stability and the change of decomposition mode were derived from the C–O–C bridges formed by the chemical crosslinking between MF and PVA and the strong interface interaction between MF and PVA.[33]

In addition, it can be seen from Fig. 7 that the T_g of PVA/MF composite coating membranes was larger than that of pure PVA (T_g: 80.2 °C), and it gradually increased to 121.0 °C with the MF content rose from 3% to 8%, until the MF content was 10%, the T_g value began to drop to 119.8 °C, which revealed the same trend as XRD analysis. In general, reducing the movement of molecular chain segments and free volume would give rise to an increase in the glass transition temperature,[13] which could provide further support for the successful chemical crosslinking of MF and PVA. Meanwhile, pure PVA showed a strong endothermic peak at 173 °C corresponding to the melting of the PVA crystalline structure, but PVA/MF composite coating membranes revealed no obvious peaks in the DSC curves, which were similar to the results of the previous work.[36]
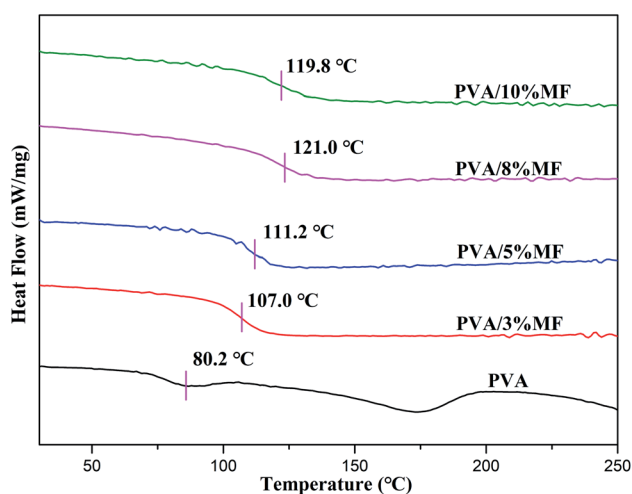

Fig. 7 DSC curves of PVA membrane and PVA/MF composite coating membranes.
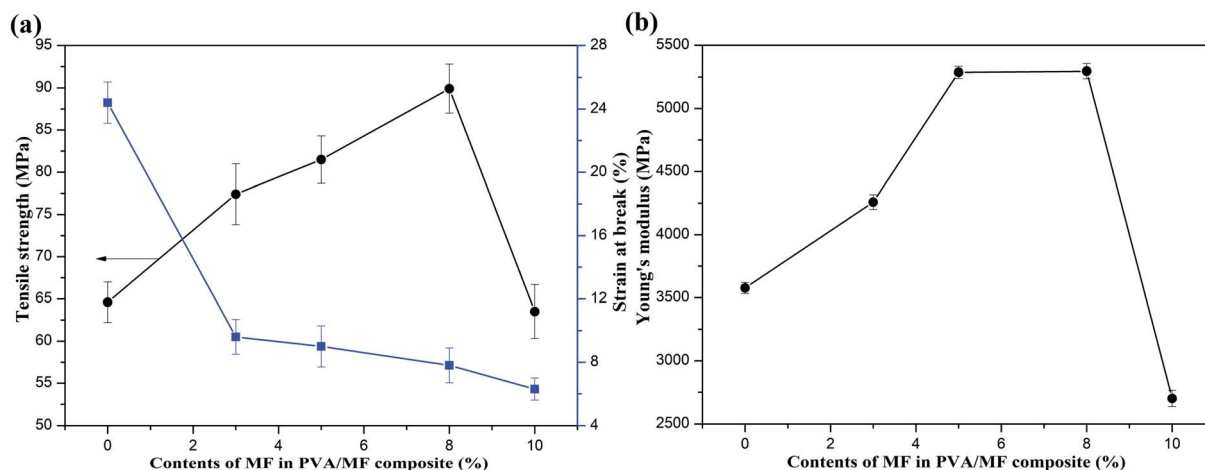
(a)

(b)

Fig. 8   Mechanical properties of PVA membrane and PVA/MF composite coating membranes.

3.4   Mechanical properties of PVA/MF composite coating membranes

Mechanical properties of PVA membrane and PVA/MF composite coating membranes are shown in Fig. 8. It can be observed that the tensile strength and Young's modulus of the pure PVA membrane were 64.6 MPa and 3576.64 MPa, respectively. The incorporation of MF into PVA has obviously changed the mechanical properties of the pure PVA membrane. With the increase of MF content in PVA/MF composite coating membranes, the tensile strength and Young's modulus significantly increased, while the elongation gradually decreased. However, when the MF addition amount reached up to 10%, the data started to reverse due to the self-condensation of MF that destroyed the PVA molecular packing density. When the MF addition amount was low, the MF mainly existed in the amorphous region of PVA, and would not penetrate into the crystalline region of PVA, so the cross-linking and curing process did not affect the crystalline behavior of PVA. When the MF addition amount reached up to 10%, in addition to the chemical reaction between MF and PVA during the thermal curing process, there would be self-condensation between its own molecules to form methylene bridges and methylene ether bridges.[31] The aggregated structure formed by the self-condensation of MF would destroy the composite hydrogel structure and increase the distance between the PVA molecular chains, affecting the chemical structure and tensile properties of PVA, which led to the decline in modulus and strength of PVA/10% MF even lower than neat PVA. It can be accepted that the linear PVA easily slid by one another *via* an outer force, so PVA possessed a low tensile strength and high elongation.[28] The incorporation of MF into PVA gave rise to the enhancement of crosslinking through the C–O–C bonding and strong interface interaction between MF and PVA that was beneficial to improving its mechanical properties.[33]

3.5   Hazes and OTRs of PVA/MF composite coating membranes

The degree of hydrolysis of the selected PVA was as high as 98.9–99%, because the partially hydrolyzed PVA contained residual acetate groups which would limit the formation of hydrogen bonds with adjacent –OH, resulting in the enhanced solubility, water absorption and permeability of PVA.[10,28,45] The hazes and OTRs of PVA/MF composite coating membranes are displayed in Fig. 9. It can be seen from Fig. 9a that the PVA/MF composite coating membranes exhibited superior transparency, which was almost the same as the haze of the BOPET or PLA substrate. This was due to the good compatibility of PVA and MF, and the PVA/MF composite coating membranes had good wettability and leveling properties on the two substrates, which could be confirmed from the SEM observation. XRD and thermal analyses showed that a small amount of MF crosslinked PVA would not affect the orderly crystallization of PVA, but could increase the glass transition temperature and thermal performance, so the PVA/MF composite coating membranes were expected to have good gas barrier properties.

The OTRs of MF/PVA composite coated BOPET and PLA membranes were compared and analyzed through the detection of OTR under different humidity conditions. As can be seen from Table 1, the OTRs of BOPET and PLA base substrates were 132.5 cm^3 per m^2 per day and 980.60 cm^3 per m^2 per day, respectively. Coating a layer of PVA coating with the thickness of 1 μm on the corona surface of the substrate could effectively improve the barrier performance. However, as the humidity increased, the OTR increased significantly. The OTR of the PVA coated BOPET membrane would increase 28 times from 50% RH to 90% RH, and correspondingly, the PVA coated PLA membrane would increase by 9 times. This was due to the fact that, in a humid environment, PVA gradually absorbed water molecules, and the hydrogen bond between its internal hydroxyl groups was weakened, resulting in a change in the aggregate structure of the PVA molecular chains and eventually expansion.[46]

However, after coating the MF/PVA composite onto BOPET and PLA membranes, the OTRs of the resultant MF/PVA composite coated BOPET and PLA membranes under high humidity conditions have been greatly improved, and the OTRs under 75% RH could still maintain at about 1 cm^3 per m^2 day,
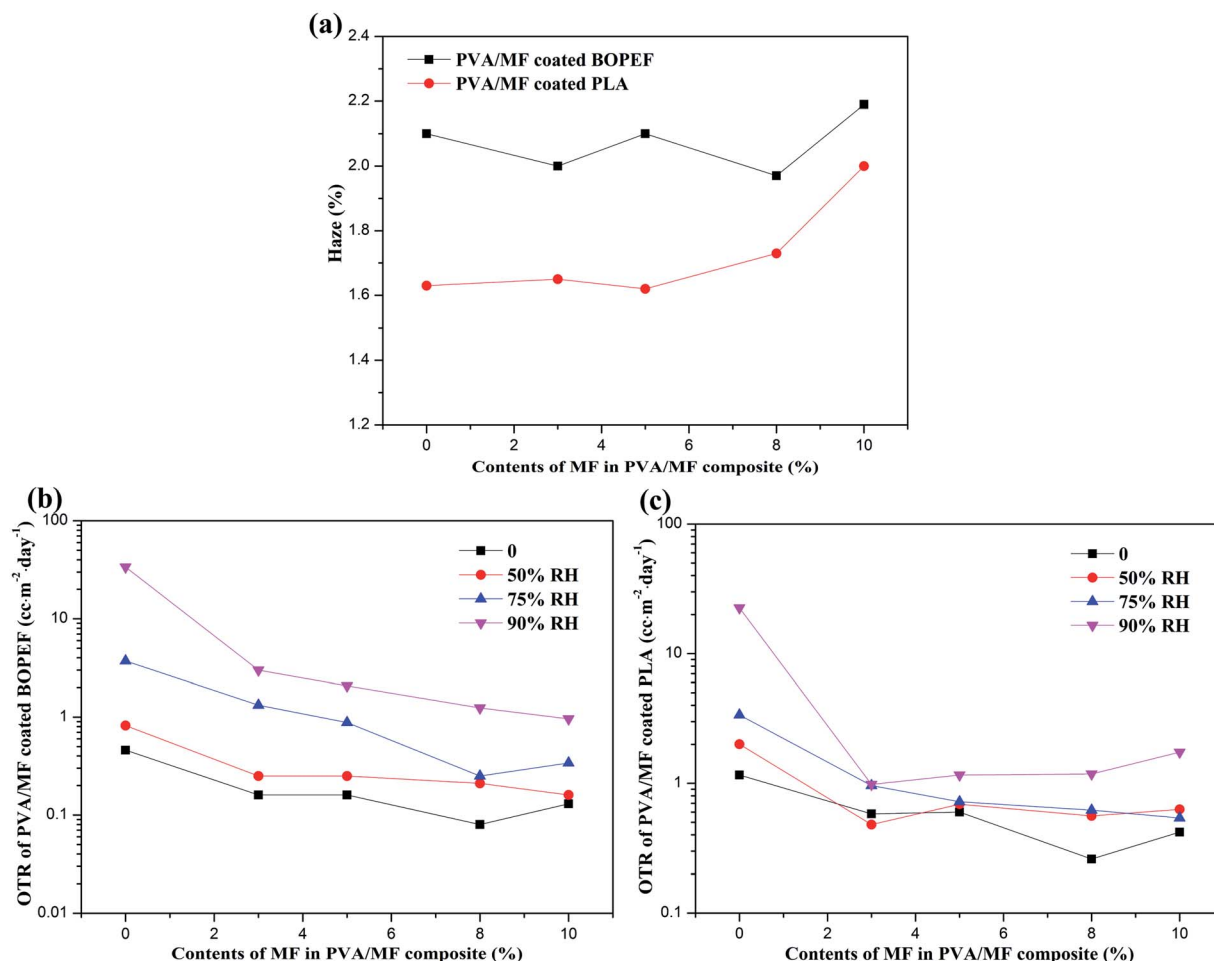
Fig. 9 (a) Hazes of PVA/MF composite coated BOPEF membranes and PVA/MF composite coated PLA membranes; (b) OTRs of PVA/MF composite coated BOPEF membranes; (c) OTRs of PVA/MF composite coated PLA membranes.

Table 1 OTRs and haze of the PVA/MF coated BOPET

Sample	OTR (cm³ per m² per day)				Haze (%)
	0% RH	50% RH	75% RH	90% RH	
BOPET	132.50	125.18	141.53	133.52	1.83
BOPET–PVA	0.46	0.82	3.72	33.72	2.10
PLA	980	—	—	—	1.58
PLA–PVA	1.16	2.01	3.38	22.54	1.63

as shown in Fig. 9b and c. With the MF content rose from 3% to 8%, the OTR improvement of the PVA/MF composite coated BOPEF and PLA membranes was not significant, and when the MF addition amount reached up to 10%, their OTRs rose again, which was also in agreement with the results of XRD and DSC analyses. These results indicated that when a small amount of MF was added, the PVA/MF composite coating could improve the moisture resistance and greatly improve the barrier properties under high humidity. There were very few research reports on the application of MF chemically crosslinked PVA for oxygen barrier coatings for food flexible packaging. Table 2 shows the comparison results of current work and literature. It is found that the oxygen barrier properties of PVA/MF composite coatings were better than other reported results.

Table 2 Comparison of OTRs of cross-linked PVA coated films/membranes with literature

Materials	Technique	Substrate/thickness of dry coating	OTR (cm³ per m² per day)		References
			25 °C, 0% RH	25 °C, 90% RH	
MF cross-linked PVA coated film	Bar-coating and drying	BOPET/1 µm	0.08–0.16	0.96–3.0	Present work
MF cross-linked PVA coated film	Bar-coating and drying	PLA/1 µm	0.54–0.96	0.98–1.74	Present work
GA cross-linked PVA coated film	Dipping and drying	BOPET/0.59 nm	14.8	—	8
GA cross-linked PVA coated film	Dipping and drying	PLA/0.59 nm	7.4	—	8
BA cross-linked PVA membrane	Coating and drying	—/60 µm	0.15–3.76	—	28

4 Conclusion

In this work, in order to decrease the sensitivity of PVA to moisture, the PVA/MF composite coating membranes with various contents of MF were successfully prepared by chemical crosslinking method. The morphology, chemical structure, thermal, mechanical properties and barrier properties of the resultant PVA/MF composite coating membranes were characterized and evaluated. The characterization results indicated that –OH in the molecular chain of MF and PVA could be crosslinked at room temperature to form a dense polymeric structure, resulting in the increase in viscosity and the decline in water absorption. And the PVA/MF composite coating had very good leveling and wettability on both BOPET and PLA substrates by roller coating, which provided a very effective way for its packaging application. The incorporation of MF into PVA gave rise to the enhancement of crosslinking, thermal stability, mechanical properties and barrier properties through the C–O–C bonding and strong interface interaction between MF and PVA. Meanwhile, the fabricated PVA/MF composite coating membranes exhibited superior transparency, improved moisture resistance and barrier properties under high humidity conditions, and the OTRs under 75% RH could still maintain at about 1.0 cm^3 per m^2 per day. On the basis of these merits, the PVA/MF composite coating membranes could exhibit great potentials for application in food flexible packaging field.

Conflicts of interest

There are no conflicts to declare.

Acknowledgements

References

1 A. Dey and S. Neogi, *Trends Food Sci. Technol.*, 2019, **90**, 26–34.

2 J. Lange and Y. Wyser, *Packag. Technol. Sci.*, 2003, **16**, 149–158.

3 Z. Zhang, I. J. Britt and M. A. Tung, *J. Appl. Polym. Sci.*, 2001, **82**, 1866–1872.

4 M. Muramatsu, M. Okura, K. Kuboyama, T. Ougizawa, T. Yamamoto, Y. Nishihara and Y. Kobayashi, *Radiat. Phys. Chem.*, 2003, **68**, 561–564.

5 A. G. Erlat, R. J. Spontak, R. P. Clarke, T. C. Robinson, P. D. Haaland, Y. Tropsha and E. A. Vogler, *J. Phys. Chem. B*, 1999, **103**, 6047–6055.

6 V. R. Tobin, H. Suttle and H. E. Assender, *Thin Solid Films*, 2017, **642**, 142–150.

7 Y. Zhao, C. Huang, X. Huang, H. Huang, H. Zhao, S. Wang and S. Liu, *Food Packag. Shelf Life*, 2020, **25**, 100513.

8 F. Ding, J. Liu, S. Zeng, Y. Xia, K. M. Wells, M. P. Nieh and L. Sun, *Sci. Adv.*, 2017, **3**, e1701212.

9 S. Mallakpour, A. Abdolmaleki and Z. Khalesi, *Polym. Bull.*, 2017, **75**, 1473–1486.

10 Z. W. Abdullah, Y. Dong, I. J. Davies and S. Barbhuiya, *Polym.-Plast. Technol. Eng.*, 2017, **56**, 1307–1344.

11 M. Dabbaghianamiri, E. M. Duraia and G. W. Beall, *Results in Materials*, 2020, **7**, 100101.

12 W. Rahman, L. T. Sin, A. Rahmat and A. Samad, *Carbohydr. Polym.*, 2010, **81**, 805–810.

13 B. Ramaraj, *J. Appl. Polym. Sci.*, 2006, **103**, 1127–1132.

14 S. Mangaraj, T. K. Goswami and P. V. Mahajan, *Food Eng. Rev.*, 2009, **1**, 133–158.

15 M. Lim, D. Kim and J. Seo, *Macromol. Res.*, 2014, **20**, 1096–1103.

16 A. Gautam and P. Komal, *J. Nanosci. Nanotechnol.*, 2019, **19**, 8071–8077.

17 C. Rovera, M. Ghaani and S. Farris, *Trends Food Sci. Technol.*, 2020, **97**, 210–220.

18 Y. Cui, S. I. Kundalwal and S. Kumar, *Carbon*, 2016, **98**, 313–333.

19 J. T. Chen, Y. J. Fu, Q. F. An, S. C. Lo, Y. Z. Zhong, C. C. Hu and J. Y. Lai, *Carbon*, 2014, **75**, 443–451.

20 B. Bolto, T. Tran, M. Hoang and Z. Xie, *Prog. Polym. Sci.*, 2009, **34**, 969–981.

21 E. Rynkowska, K. Fatyeyeva, S. Marais, J. Kujawa and W. Kujawski, *Polymers*, 2019, **11**, 1799.

22 W. Ji, N. U. Afsar, B. Wu, F. Sheng, M. A. Shehzad, L. Ge and T. Xu, *J. Membr. Sci.*, 2019, **590**, 117267.

23 S. Xu, L. Shen, C. Li and Y. Wang, *J. Appl. Polym. Sci.*, 2018, **135**, 46159.

24 J. Wang, X. Wang, C. Xu, M. Zhang and X. Shang, *Polym. Int.*, 2011, **60**, 816–822.

25 A. L. Ahmad, N. M. Yusuf and S. B. Ooi, *Desalination*, 2012, **287**, 35–40.

26 K. C. S. Figueiredo, T. L. M. Alves and C. P. Borges, *J. Appl. Polym. Sci.*, 2009, **111**, 3074–3080.

27 G. Leone, *J. Mater. Sci.: Mater. Med.*, 2010, **21**, 2491–2500.

28 M. Lim, H. Kwon, D. Kim, J. Seo, H. Han and S. B. Khan, *Prog. Org. Coat.*, 2015, **85**, 68–75.

29 R. C. Wilson and W. F. Pfohl, *Vib. Spectrosc.*, 2000, **23**, 13–22.

30 S. H. Imam, S. H. Gordon, L. Mao and L. Chen, *Polym. Degrad. Stab.*, 2001, **73**, 529–533.

31 V. N. Pavlyuchenko, S. S. Ivanchev, M. Rätzsch, H. Bucka, O. N. Primachenko, P. Leitner and S. Y. Khaikin, *J. Appl. Polym. Sci.*, 2006, **101**, 2977–2985.

32 H. R. Asemani and V. Mannari, *Prog. Org. Coat.*, 2019, **131**, 247–258.

33 C. Yu, W. Xu, X. Zhao, J. Xu and M. Jiang, *Fibers Polym.*, 2014, **15**, 1828–1834.

34 L. L. Li, Y. Q. Kang, Y. G. Yang, R. M. Cong and Z. Jia, *Adv. Mater. Res.*, 2015, **1088**, 419–423.

35 R. Kakkar, K. Madgula, Y. V. S. Nehru and J. Kakkar, *Eur. Chem. Bull.*, 2015, **4**, 98–105.

36 K. Shang, J. C. Yang, Z. J. Cao, W. Liao, Y. Z. Wang and D. A. Schiraldi, *ACS Appl. Mater. Interfaces*, 2017, **9**, 22985–22993.

37 K. E. Strawhecker and E. Manias, *Chem. Mater.*, 2000, **12**, 2934–2949.

38 A. Hasimi, A. Stavropoulou, K. G. Papadokostaki and M. Sanopoulou, *Eur. Polym. J.*, 2008, **44**, 4098–4107.

39 I. C. McNeill, *J. Anal. Appl. Pyrolysis*, 1997, **40–41**, 21–41.

40 A. I. Cano, M. Cháfer, A. Chiralt and C. González-Martínez, *Polym. Degrad. Stab.*, 2016, **132**, 11–20.

41 A. Abdolmaleki, S. Mallakpour and S. Borandeh, *Polym. Compos.*, 2016, **37**, 1924–1935.

42 H. Q. Yan, X. Q. Chen, M. X. Feng, Z. F. Shi, W. Zhang, Y. Wang, C. R. Ke and Q. Lin, *Colloids Surf., B*, 2019, **177**, 112–120.

43 H. Q. Yan, X. Q. Chen, C. L. Bao, J. L. Yi, M. Y. Lei, C. R. Ke, W. Zhang and Q. Lin, *Colloids Surf., B*, 2020, **191**, 110983.

44 H. L. Kang, Y. Shu, Z. Li, B. Guan, S. J. Peng, Y. Huang and R. G. Liu, *Carbohydr. Polym.*, 2014, **100**, 158–165.

45 X. Tang and S. Alavi, *Carbohydr. Polym.*, 2011, **85**, 7–16.

46 J. M. Kim, M. H. Lee, J. A. Ko, D. H. Kang, H. Bae and H. J. Park, *J. Food Sci.*, 2018, **83**, 349–357.